DNAzyme-templated exponential isothermal amplification for sensitive detection of lead pollution and high-throughput screening of microbial biosorbents

Hao Yang[a], Yumei Liu[a], Yi Wan[b], Yi Dong[a], Qiang He[a], Mohammad Rizwan Khan[c], Rosa Busquets[d], Guiping He[a], Jiaqi Zhang[a], Ruijie Deng[a], Zhifeng Zhao[a,*]

[a] College of Biomass Science and Engineering, Healthy Food Evaluation Research Center and Key Laboratory of Food Science and Technology of Ministry of Education of Sichuan Province, Sichuan University, Chengdu 610065, China

[b] Key Laboratory of Tropical Biological Resources of Ministry of Education, School of Life and Pharmaceutical Sciences, Marine College, State Key Laboratory of Marine Resource Utilization in South China Sea, Hainan University, Haikou 570228, China

[c] Department of Chemistry, College of Science, King Saud University, Riyadh, 11451, Saudi Arabia

[d] School of Life Sciences, Pharmacy and Chemistry, Kingston University, KT1 2EE Kingston Upon Thames, United Kingdom

* Corresponding authors:

e-mail: zhaozhifeng@scu.edu.cn

Abstract

Very low concentrations of lead (Pb^{2+}) pollution can have far-reaching adverse impacts on human health, due to the cumulative toxicity of Pb^{2+}. Herein, we report a DNAzyme-templated exponential isothermal amplification strategy (termed DNAzymee) for the ultrasensitive detection of Pb^{2+} pollution and the high-throughput screening of microbial biosorbents to remove Pb^{2+} pollution. DNAzyme can specifically recognize Pb^{2+}, and this recognition event can be amplified by the subsequent exponential isothermal amplification reaction (EXPAR) and monitored by a G-quadruplex specific dye. The proposed design showed a low limit of detection (95 pM) and could identify Pb^{2+} pollution in different real samples with high precision. In particular, the proposed assay was used to screen Pb^{2+} biosorbents, and the results showed that *Leuconostoc mesenteroides* is a promising microbial biosorbent for removing Pb^{2+} pollution. Thus, the DNAzymee assay can serve as a platform to monitor lead pollution in the environment and screen efficient biosorbents for the control of lead pollution.

Keywords: lead poolution, environmental safety, DNAzyme, G-quadruplex, biosorbent

1. Introduction

Lead ions (Pb^{2+}) are nonessential metal ions that are toxic even at low levels of exposure, and are not subject to biodegradation (Ashraf et al., 2020; Malavolti et al., 2020). Ubiquitous contamination of Pb^{2+} in the environment, especially in water, resulting from the mining industry, recycled gasoline, and road dust, has adverse effects on human health. The chronic toxicity of Pb^{2+} causes genotoxicity and neurotoxicity, even when low levels of Pb (less than 10 μg/mL) are present in the blood (Balasubramanian et al., 2020). Thus, Pb^{2+} pollution must be controlled at a very low level. Biosorbents are well known for their outstanding performance in the biosorption of heavy metals, and thus, have the potential to remove Pb^{2+} in complex real samples. Other removal methods that have been reported, include membrane separation (Roy Choudhury et al., 2018), reverse osmosis (Corroto et al., 2019), and filtration (Kang et al., 2019). Among the methods, microbial biosorbents are advantageous due to their low cost, ability to work under a wide range of pH conditions, and rapid regeneration; in particular, microbial biosorbents exhibit an outstanding metal ion biosorption efficiency (Concórdio-Reis et al., 2020; Rasmey et al., 2018). Microbial biosorbents that have been reported include Lactobacillus brevis (Dai et al., 2019), Ralstonia solanacearum (Pugazhendhi et al., 2018), Leuconostoc mesenteroides (Yi et al., 2017) and Bacillus xiamenensis (Mohapatra et al., 2019). The high toxicity with a low threshold, and the ubiquity of lead pollution result in high demands for the development of sensitive Pb^{2+} assays, which would benefit both lead pollution monitoring and biosorbent screening.

The standard methods for Pb^{2+} detection including atomic absorption spectroscopy, inductively coupled plasma-mass spectrometry, and flame atomic absorption spectrometry are precise and

have high repeatability. These tools play key roles in assessing lead pollution. However, they are inefficient for the detection of trace amounts of Pb^{2+} and typically require expensive equipment, professional technicians, and long detection times (several hours to days); thus, these methods are unsuitable for widespread application, especially in low-resource settings. Molecular analytical technologies are potential choices to address these shortcomings (Rao et al., 2021).

Deoxyribozymes (also referred to as DNAzymes) are synthetic single-stranded DNA molecules with catalytic activity that is triggered by specific cofactors, such as metal ions (Pb^{2+}, UO_2^{2+}, Cu^{2+} and Ag^{+}), thus enabling the development of tailor-made DNAzymes for the detection of specific metals (Saran and Liu, 2016; Shan et al., 2019; Yang et al., 2022; Yang et al., 2021). Due to their features of low cost, high stability, remarkable specificity and flexibility of design, the use of DNAzymes as key components for biosensing is rapidly increasing. The first Pb^{2+}-dependent DNAzyme was obtained by in vitro selection (Breaker and Joyce, 1994). Of the two common Pb^{2+}-specific DNAzymes available today, GR-5 DNAzyme exhibits an ~40,000-fold higher selectivity than 8–17 DNAzyme (Lan et al., 2010); thus, GR-5 DNAzyme was used in this work. The combination of DNAzyme-based biosensors with nucleic acid amplification strategies (Chen et al., 2020; Feng et al., 2021; Liu et al., 2020), such as rolling circle amplification and exponential isothermal amplification reaction (EXPAR), can enhance their sensitivity in assays.

Herein, we report a DNAzyme-templated exponential isothermal amplification strategy (termed DNAzymee) for the highly sensitive detection of lead ions in real samples and the high-throughput screening of microbial biosorbents that are capable of removing lead

pollution. DNAzyme can specifically recognize Pb2+, and this recognition event can be amplified by the subsequent EXPAR reaction and monitored using G-quadruplex-specific dyes. Utilization of EXPAR amplification enables the proposed DNAzymee assay to exhibit high sensitivity to limit of detection (LOD) of 95 pM. The DNAzymee assay could reliably identify trace lead pollution in food and environmental samples. In particular, the proposed assay was applied to screen Pb^{2+}-tolerant biosorbents, and the results showed that Leuconostoc mesenteroides (L. mesenteroides) is a promising microbial biosorbent for removing lead pollution.

2. Materials and methods

2.1. Reagents and materials

Oligonucleotide sequences are summarized in Table S1 and purchased from Sangon (Shanghai, China). The substrate strand was HPLC purified, the other sequences were PAGE purified. $Pb(CH_3COO)_2$ was obtained from Sigma (Mississauga, ON, Canada). *N*-methyl Mesoporphyrin IX (NMM) was bought from Santa Cruz Biotechnology, Inc. (Dallas, USA). HEPES (2-[4-(2-hydroxyethyl) piperazin-1-yl] ethanesulfonic acid), $MgCl_2$ and NaCl were obtained from Alfa Aesar by fv (Shanghai, China), Tris-HCl was obtained from Sangon (Shanghai, China). $CoCl_2$, Mn $(CH_3COO)_2$, Cd $(NO_3)_2$, Al $(NO_3)_3$, $CuSO_4$, $NiCl_2$, KCl, HNO_3, and $HClO_4$ were obtained from Kelon (Chengdu, China). 10 mM of deoxynucleotide (dNTP) Solution Mix (No. N0447L) and 10 U/μL nicking endonuclease (Nt.BbvcI, No. R0632L) were obtained from New England Biolabs Ltd. (Whitby, ON, Canada). 5 U/μL Klenow Fragments (exo^-) (No. EP0422) and 10× Klenow Buffer were obtained from Thermo

Fisher Scientific (Mississauga, ON, Canada). Agarose, 50× Tris-acetate-EDTA buffer, and 10,000× Gel Red dye were purchased from Beijing Ding Guo Biotechnology Co., Ltd. (Beijing, China). 6× loading buffer was purchased from Tsingke Biological Technology Co., Ltd. (Beijing, China). MRS Broth and Nutrition Broth were purchased from Qingdao Hope Bio-Technology CO., Ltd. (Qingdao, China). Molecular biological water was obtained from Corning Co., Ltd. (New York, USA).

2.2. Pb^{2+} detection

The proposed DNAzymee assay was composed of DNAzyme cleavage reaction and EXPAR amplification. First, the cleavage reaction proceeded with 4 μL of 10× reaction buffer (500 mM HEPES, 500 mM NaCl, 50 mM $MgCl_2$, pH 7.26) according to Deng's study (Deng et al., 2018), 1 μL of 4 μM substrate strand, 1 μL of 4 μM DNAzyme strand and 1 μL of different concentrations of Pb^{2+}, after 30 min incubation at room temperature, the EXPAR proceeded by adding 1 μL of 4 μM P_1,1 μL of 4 μM P_2, 1 μL of 12 μM Blocker DNA, 3 μL of 10 mM dNTPs, 4 μL of 10× Klenow Buffer, 0.5 μL of 5 U/μL Klenow Fragments (exo^-), 0.5 μL of 10 U/μL Nt.BbvCI and 4 μL of 20 μM NMM to the cleavage reaction mixture, then 18 μL H_2O was added to make a total volume of 40 μL. After incubation at 37 °C for 30 min, the enzymes were inactivated at 85 °C for 15 min, then 40 μL of the mixture was taken to perform the fluorescence signaling with the microplate reader Synergy H1 (Biotek, USA).

2.3. Fluorescent recording

The fluorescence of NMM was collected at the emission wavelength ranging from 550 nm to 700 nm with the excitation wavelength of 399 nm. For dynamic fluorescence analysis, the

temperature was set to 37 °C in advance and the fluorescence of NMM was collected every minute, the total detection time was 1 h, right after adding Klenow Fragments (exo$^-$) and Nt.BbvCI.

2.4. Electrophoresis analysis

For electrophoresis analysis, 6 μL mixture including 1 μL of 6× loading buffer and 5 μL of oligonucleotides was prepared in advance. 50 ml agarose gel was prepared with 2.5 % agarose, 1× TAE buffer and 1× Gel Red dye. Agarose gel electrophoresis was carried out in 1× TAE buffer at 90 V for 50 min, after which the gel was immediately visualized via the Gel Doc XR+ system (BioRad, USA).

2.5. Detection of Pb^{2+} in real complex samples

Fresh eggs and pear juice were primed in advance and stored at 4 °C until use, and tap water was collected on the Sichuan University campus. Eggs and pear juice were obtained from a supermarket (Chengdu, China). Before the spike-recovery test, fresh eggs were prepared with a digestive process. First, 0.5 ml of liquid egg was added to a digestion tube followed by 10 mL of HNO_3, and 0.5 mL of $HClO_4$; this mixture was digested according to the Chinese National Standard for Food Safety - Determination of Lead Content in Food Products (GB 5009.12-2017, in Chinese): 120 °C for 1 h, 180 °C for 3 h, 200 °C for 1 h. Then, ultrapure water was added to the colorless residue to adjust the total volume to 10 mL. After adjusting the pH of the solution to approximately 7.0, different concentrations of Pb^{2+} were added to the solution for detection. Pear juice was also used as a sample for Pb^{2+} analysis.

2.6. Screening of biosorbents

Bacteria can serve as promising reagents for removing heavy metal pollution (Halttunen et al., 2007; Pakdel et al., 2019). The biosorption rate was evaluated using the proposed platform to characterize potential strains for Pb^{2+} biosorption and determine the optimal pH condition. The biosorption efficiency C (%) was assessed by the following formula (Yang et al., 2021):

$C\%=A_0-A/A_0\times100\%$

where A and A_0 represent the final and initial concentrations of Pb^{2+} in the biosorption solution, respectively.

Ten bacteria were selected for investigating Pb^{2+} removal (Table S2). Some of these bacteria were isolated from Chinese horse bean-chili-paste (Lu et al., 2020), and the MiSeq sequencing data were deposited in the NCBI Sequence Read Archive; the other bacteria were the type strains that are typically used for research. The counted bacteria were centrifuged at 12,000 rpm for 15 min, after which the precipitate was washed with 0.9 % brine three times. The precipitate was inactivated at 121 °C for 15 min and freeze-dried at −54 °C to generate a bacterial powder. The powder was made by thoroughly grinding the freeze-dried bacteria and stored at −20 °C until use. For the screening of biosorbents, a 10 g/L bacterial solution was prepared with each bacterial powder and diluted to 10^8 CFU/ml. First, the inactivated bacterial powder of 10 strains were used to artificially contaminated pear juice, and the biosorption conditions were 30 °C, 150 r/min, and 1 h. Then, the processed filtrate was analyzed by the DNAzymee assay to assess the biosorption efficiency.

2.7. Bacterial culture and counting

The bacterial lyophilized powders were prepared with the same method as Li's (Li et al., 2020). For cultural of *L. mesenteroides*, *E. faecium*, *L. lactis* subsp. *lactis*, *W. hellenica* and *T. halophiles*, they were activated in a 200 mL MRS medium at 37 °C for 24 h first, then 1 mL activated bacteria liquid was introduced to a new 200 ml MRS culture for proliferation at 37 °C for 24 h. Solid MRS medium was also prepared for bacteria counting, 50 μL of the serial dilution were flatly coated at the solid medium and incubated at 37 °C for 48 h, usable bacterial colonies (30–300) were utilized to estimate the total colonies. The preparation of lyophilized powders of *B. subtilis*, *B. licheniformis* and *B. amyloliquefaciens* were the same as above (Li et al., 2020). The difference was the medium changing to NB broth.

2.8. Characterization of cellular morphology

After Pb^{2+} biosorption at 30 °C for 1 h, the samples were vacuum filtered with a 0.22 μm membrane and washed three times with ultrapure water. The washed microporous membranes were dried naturally for approximately 1 h and then cut into 5 mm^2 squares for FESEM (Field emission scanning electron microscopy) with an Apreo S HiVoc SEM (Thermo Fisher Scientific, Shanghai, China) with an accelerating voltage of 5.00 kV to investigate surface morphology. The samples were covered with Au before FESEM. In addition, the lyophilized microbial biosorbents were analyzed by KBr pressed-disc-based Fourier Transform Infrared Spectroscopy (FTIR, INVENIO R, Germany) to characterize the interactions between the biosorbents and lead. The IR spectral range was set to 4000–400 cm^{-1} with a resolution of 4 cm^{-1} (Li et al., 2020).

3. Results and discussion

3.1. Working principles

The label-free DNAzymee assay consists of three processes: DNAzyme recognition, EXPAR amplification, and G-quadruplex signaling (Fig. 1). The substrate strand comprises a riboadenosine (rA). The probes P_1 and P_2 are the primer and the template for the EXPAR reaction, respectively. The P_1 probe is composed of a recognition region that hybridizes to the substrate strand and a primer region. The P_2 probe contains four parts: (i) a recognition sequence complementary to the substrate strand; (ii) an anti-primer sequence complementary to the primer region of the P_1 probe; (iii) a nicking cleavage site acted upon by Nt.BbvCI endonuclease; and (iv) a template region of G-quadruplex. With the addition of Pb^{2+}, the DNAzyme strand is activated to mediate the multiple-turnover cleavage of the substrate strand at the rA site. Sequential DNAzyme-templated EXPAR amplification cannot occur due to breakage of the substrate strand. In the absence of Pb^{2+}, the intact substrate strand can trigger the assembly of a three-way junction structure (substrate–P_1–P_2) that enables the initiation of the sequential EXPAR amplification, producing abundant G-quadruplex molecules. The resultant G-quadruplex molecules can illuminate the G-quadruplex-specific dye NMM. The dual amplification via multiple-turnover cleavage of DNAzyme and the EXPAR reaction endows the DNAzymee assay with a high sensitivity for Pb^{2+} detection. The adoption of a G-quadruplex probe eliminates the need for nucleic acid probes with chemical labels. The proposed DNAzymee assay was further successfully used to screen microbial biosorbents to remove lead pollution.

Fig. 1. Scheme of the DNAzymee assay for detecting Pb^{2+} and screening biosorbents.

Fluorescence analysis was first used to investigate the feasibility of the DNAzymee assay (Fig. 2A). The G-quadruplex sequence could activate the fluorescence of NMM dye (line 1). The substrate-templated proximity of EXPAR probes resulted in a high fluorescence (line 2), indicating the production of high amounts of the G-quadruplex sequences. There was a trade-off in fluorescence output when the DNAzyme strand was added (line 3), probably due to the competition of the DNAzyme-substrate duplex with the substrate-P_1-P_2 complex. Lack of Nt.BbvcI (line 4), Klenow Fragments (exo^-) (line 5), or both (line 6), led to a fluorescence close to that of the background, indicating that both Nt.BbvcI and Klenow Fragments (exo^-) are necessary for the EXPAR reaction. Upon the addition of Pb^{2+}, the fluorescent signal of NMM dramatically decreased due to the target-specific triggering of substrate strand cleavage (line 7).

Electrophoresis was further used to verify the principle of the DNAzymee assay (Fig. 2B and C). As verification of DNAzyme cleavage (Fig. 2B), lane 3 clearly lagged behind lane 1, and lane 2 suggested the formation of a DNAzyme-substrate duplex. The addition of Pb^{2+} resulted in cleavage of the substrate strand, which produced a 9-nt fragment and disassembly of the above duplex, as the band obviously moved forward in lane 4 and kept pace with that in lane 6. As verification of the EXPAR probes (Fig. 2C), the lag of lane 5 compared to lane 2 demonstrated proximity hybridization between P_1 and P_2 templated by the substrate strand. As seen in lane 6, DNAzyme did not impact the production of G-quadruplex, which was consistent with the fluorescence analysis in Fig. 2A. The lack of Nt.BbvcI and Klenow Fragments (exo^-) can hinder the occurrence of EXPAR (lane 6).

3.2. Optimization of the DNAzymee assay

Formation of the three-way junction is critical for the DNAzymee assay; thus, the length of the recognition arms of P_1–P_2 was first optimized (Fig. S1), and the arm length of 10–10 nt exhibited the optimal signal response. Dynamic fluorescence analysis was carried out to determine the reaction kinetics of EXPAR in the detection of Pb^{2+} without consideration of the negligible binding time of NMM dyes and G-quadruplex (Fig. S2). The fluorescence measured at 612 nm gradually increased in the absence of Pb^{2+} within 30 min, while the fluorescence after the addition of Pb^{2+} remained similar to the background level (Fig. 3A), revealing rapid EXAPR amplification. Therefore, 30 min of EXPAR reaction time was used for subsequent experiments. The hybridizing stability between the DNAzyme and substrate strand could regulate the conversion of the DNAzyme cleavage. Five hybridization arms with different lengths ranging from 5–5 nt to 9–9 nt were selected (Table S1). As the arm length increased, the difficulty in forming the three-way junction increased. The weak binding of the DNAzyme strand to the substrate strand led to a high background, while the strong binding resulted in a low signal. The optimization showed that the arm length of 7–7 nt resulted in the highest background-signal ratio (B/S ratio) (Fig. 3B). Given that blocking the spontaneous formation of the three-way junction could reduce the background, we devised a blocker DNA complementary to the primer for EXPAR (P_1). The optimal B/S ratio was achieved when the concentration of blocker DNA was set to 300 nM (Fig. 3C), and it is noteworthy that excessive blocker DNA might lead to undesirable dimers, which hindered EXPAR. We further investigated several G-quadruplexes with different capacities for the illumination of the NMM

dyes (Fig. 3D), and the sequences are provided in Table S1. The results showed that G_2 yielded the highest B/S ratio; thus, G_2 was selected for this work.

3.3. Detection performance of the DNAzymee assay

The quantitative performance of the DNAzymee assay was assessed based on the optimum experimental conditions. The fluorescence gradually decreased when the Pb^{2+} concentration increased from 0 nM to 500 nM (Fig. 4A), and it reached a saturated state when the Pb^{2+} concentration exceeded 100 nM (Fig. 4B). The fluorescence intensity showed a linear relationship with the concentration of Pb^{2+} in the range of 0.1 nM to 5 nM. The linear regression equation was calculated as $Y = -645.31X + 4245.97$ ($R^2 = 0.993$), where X and Y represent the Pb^{2+} concentration and fluorescence intensity, respectively. The LOD of the proposed assay was calculated to be 95 pM. The LOD was defined as the amount of lead ions that corresponded to the fluorescence signal of the background with the addition of three times the standard deviation. The DNAzymee assay for detecting Pb^{2+} is advanced (Table S3), mainly by the following three features: (i) dual amplifications including a DNAzyme-catalyzed multiple-turnover cleavage and a EXPAR reaction confer a high sensitivity; (ii) use of the G-quadruplex probe to enable label-free detection; and (iii) the potential for high-throughput screening of the microbial biosorbents.

Fig. 4. Detection performance of the DNAzymee assay. (A) Fluorescent spectra in the presence of different concentrations of Pb^{2+} (0, 0.1, 0.2, 0.5, 3, 5, 10, 50, 100, 300, 500 nM). (B) The corresponding calibration curve of the fluorescence versus the concentration of Pb^{2+}. (C) The

specificity of the DNAzymee assay for Pb^{2+} detection. The signal responded to various metal ions (Pb^{2+}, Cd^{2+}, Al^{3+}, Cu^{2+}, Mn^{2+}, Co^{2+}, and Ni^{2+}).

Heavy metal ions commonly found in the environment were used to test the specificity of the DNAzymee assay for Pb^{2+} detection. The selected interferent metal ions included Cd^{2+}, Al^{3+}, Cu^{2+}, Mn^{2+}, Co^{2+} and Ni^{2+}, and the concentrations were set to 50, 100, and 500 nM. Only Pb^{2+} caused an obvious signal response, while the presence of Cd^{2+}, Al^{3+}, Cu^{2+}, Mn^{2+}, Co^{2+} and Ni^{2+} resulted in a signal nearly the same as that of the blank samples (Fig. 4C and Fig. S3). The discrimination factor (DF) was used to better evaluate the selectivity of the DNAzymee assay according to Zhang's study (Zhang et al., 2021). The DFs of Cd^{2+}, Al^{3+}, Cu^{2+}, Mn^{2+}, Co^{2+} and $Ni^{2+}$to Pb^{2+} ranged from 3.39 to 293.52 (Table S4). These results showed that the proposed sensing system could reliably discriminate Pb^{2+} from other heavy metals.

3.4. Monitoring lead pollution in food and environmental samples

The development of the mining industry and urbanization have increased the pollution of Pb^{2+} in the ecological environment, in turn affecting the safety of food and drinking water. Fresh egg, which is frequently contaminated by Pb^{2+}, was selected as a sample to validate the feasibility of the DNAzymee assay for detecting lead contamination in complex real samples. A spike-recovery experiment was carried out where 1 nM, 2 nM, and 3 nM Pb^{2+} were spiked into the prepared sample solution. As shown in Fig. S4 and Table S5, the recovery rate varied from 90.4 % to 104.2 %, showing that the proposed method has the potential to detect Pb^{2+} in real environmental samples.

3.5. Screening of microbial biosorbents

Fruit juice production is susceptible to Pb^{2+} contamination during the collection, processing, and packaging of the fruit. Conventional Pb^{2+} removal approaches may cause various side effects for food and drinks; thus, new methods are urgently needed to alleviate Pb^{2+} toxicity. Bacteria are good options for heavy metal biosorption. Ten strains (Table S2) were selected, and their ability to remove Pb^{2+} was assessed using the DNAzymee assay. In principle, bacteria are capable of absorbing both metal ions and nucleic acid probes. The final concentration of DNAzyme probes that reached 1 μM, was high enough for microbial biosorbent screening. Moreover, Pb^{2+} solution after biosorption would be filtered and diluted to the applicable concentration before quantification by the DNAzymee assay, after this step, the amounts of bacteria remaining in the sample posed little risk of biosorption to nucleic acid probes. Therefore, the minimal loss of nucleic acid probes did not greatly degrade the performance of the DNAzymee assay in the quantification of lead concentration. In addition, it was necessary to dilute the lead concentration to that with the linear range (0.1–5 nM) for the subsequent lead analysis after biosorption. When the pH was set to 7.0, the solubility of Pb^{2+} was estimated to be ~6.12 ppm (~30 μM) (Inyang et al., 2016) that was much greater than the Pb^{2+} concentration used in the analysis of Pb^{2+}. Therefore, the removal of Pb^{2+} mainly depended on the adsorption by microbial biosorbents, rather than the precipitation of lead in the analysis medium (pH 7).

The process of Pb^{2+} biosorption is considered pH dependent. On the one hand, under low pH conditions, the proteins on the cell surface could expose more negatively charged groups, such as phosphate groups, that could bind to Pb^{2+}. On the other hand, the competition between

Pb^{2+} and H^{+} for negatively charged binding sites also influences the biosorption rates. Therefore, the impact of pH (2.0, 3.0, 4.0, 5.0 and 6.0) on the biosorption rate was characterized. *L. mesenteroides* showed the highest biosorption efficiency (47.71 %) when the pH was approximately 4 (Fig. 5A and Table S6). We compared the biosorption efficiency with other biosorbents (Table S7), the trade-off in lead biosorption efficiency of the proposed DNAzymee assay may be due to the complex microenvironment of fruit juice compared to water. The inactivation process could have released proteins from inside of the cell to the outside; therefore, many different possible ligands capable of the cationic binding of ions such as Pb^{2+} by inactivated bacteria were produced.

Since the natural pH of juice is close to 4 and L. *mesneteroides* is food-grade safe, it was further investigated by FESEM. FESEM was used to characterize the appearance of L. *mesenteroides* under conditions with and without Pb^{2+} (50 μM, 100 μM or 200 μM). The L. *mesenteroides* were rod-like and smooth without Pb^{2+} (Fig. 5B). With the increase in Pb^{2+} concentrations, more L. *mesenteroides* grouped together, and the surface was clearly rough; this meant that as Pb^{2+} concentrations increased, more Pb^{2+} was able to attract the negatively charged leaky intracellular proteins. Thus, *L. mesenteroides* interacted with Pb^{2+} through electrostatic interactions (Fig. 5C, D, and E). The surface change was expected since the cell membrane was mainly negatively charged and Pb^{2+} could be attracted. The results of the FESEM analysis indicated that the biosorbents had good structure, and there were abundant functional groups on the surface that could absorb Pb^{2+}. *L. mesenteroides* could be used for Pb^{2+} preconcentration at trace/ultratrace levels, thus facilitating the control of lead pollution. Furthermore, FTIR analysis was carried out at pH 7.0 to confirm the interaction of

biosorbents and lead ions. The biosorption of heavy metals mainly depends on electrostatic bonding with microbial exopolysaccharides (Morillo Pérez et al., 2008). The wide absorbance at 3284–3296 cm^{-1} indicated the –OH group (Yi et al., 2017), and the wide absorbance at 528–564 cm^{-1} showed carbon-halogen (C-X) stretching (Raevskii et al., 1973). Following the biosorption of 0 μM to 200 μM Pb^{2+}, the absorption peaks at 3284 and 528 cm^{-1} were shifted to 3288, 3296 and 3296 as well as 548, 560 and 564 cm^{-1}, respectively (Fig. 5F). These increases demonstrated the interaction of microbial biosorbents and lead.

4. Conclusion

In summary, the established DNAzymee assay combined the merits of the high specificity and sensitivity of DNAzyme and the signal amplification effect of EXPAR, and this assay could be adapted for the ultrasensitive detection of lead pollution. The use of a G-quadruplex-specific dye eliminates the need for chemically labeled nucleic acid probes which are costly and difficult to synthesize. The proposed DNAzymee assay could detect Pb^{2+} at a subpicomolar level, and the capacity to sense lead pollution in real environmental samples was validated. In particular, the DNAzymee assay allowed high-throughput screening of microbial biosorbents using a microplate reader, and *L. mesenteroides* was found to be a promising biosorbent for removing lead pollution. Therefore, the DNAzymee assay can serve as a reliable tool to facilitate lead pollution monitoring and control.

Acknowledgement

This work was financially supported by National Natural Science Foundation of China (No. 22074100), the Green Manufacturing Project of Ministry of Industry and Information Technology of China and the Researchers Supporting Project Number (No. RSP-2021/138), and King Saud University, Riyadh, Saudi Arabia.

Fig. 1. Scheme of the DNAzymee assay for detecting Pb^{2+} and screening biosorbents.

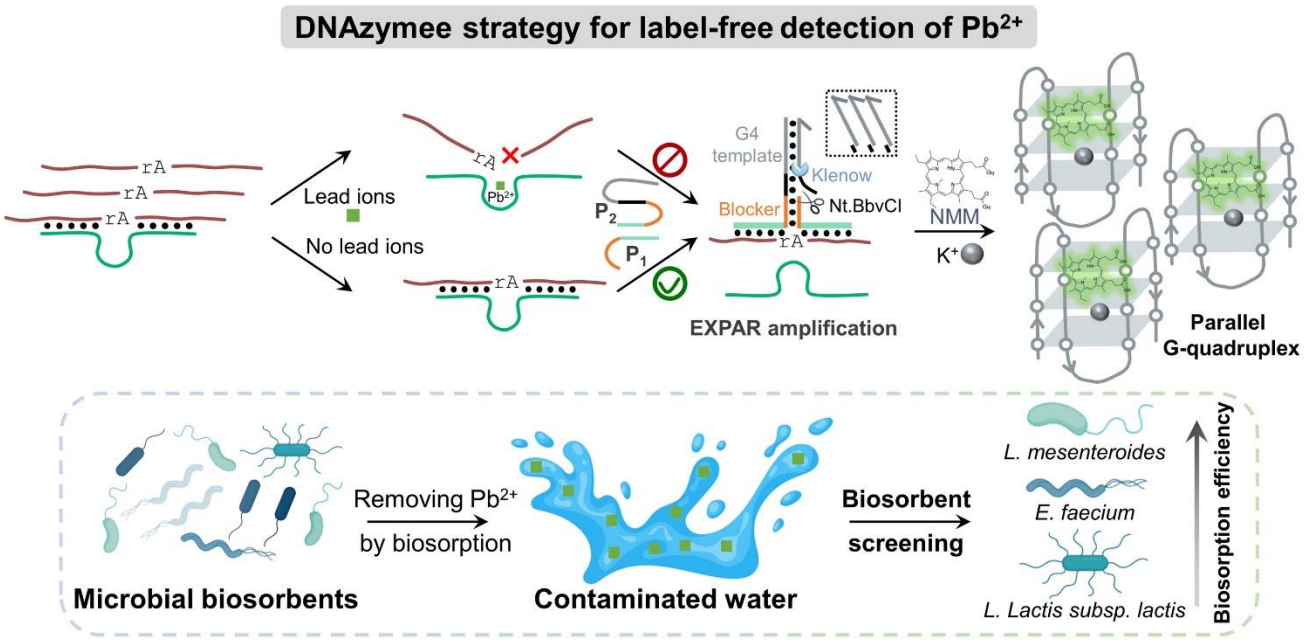

Fig. 2. Investigation the working principle of the DNAzymee assay. (A) Fluorescence analysis of the DNAzymee assay. (B) Investigation of the Pb^{2+}-activated DNAzyme cleavage using agarose gel electrophoresis. (C) Investigation of the EXPAR reaction via agarose gel electrophoresis

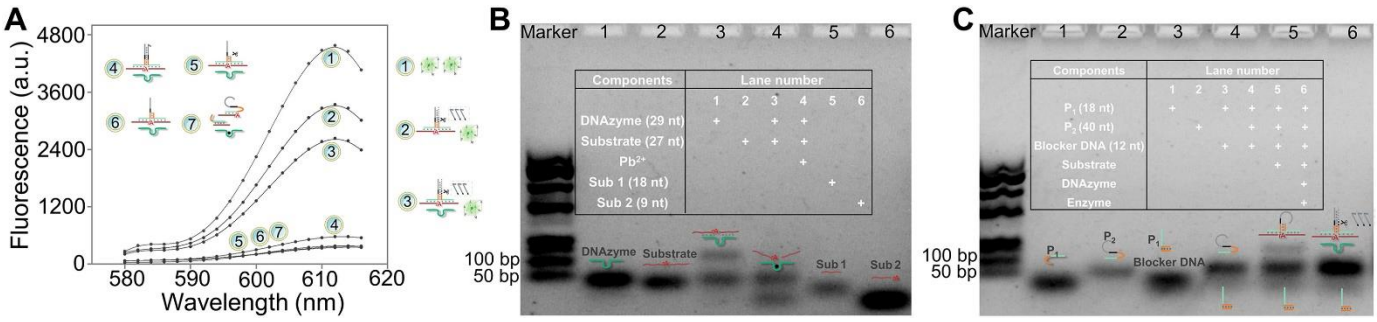

Fig. 3. Optimization of the DNAzymee assay. (A) Fluorescent dynamics in the presence and absence of Pb^{2+}. (B) Optimization of the hybridization arms (m–n) of DNAzyme strand. m and n indicate the hybridization length of each arm. (C) Optimization of the blocker DNA concentrations. (D) Screening of different G-quadruplexes.

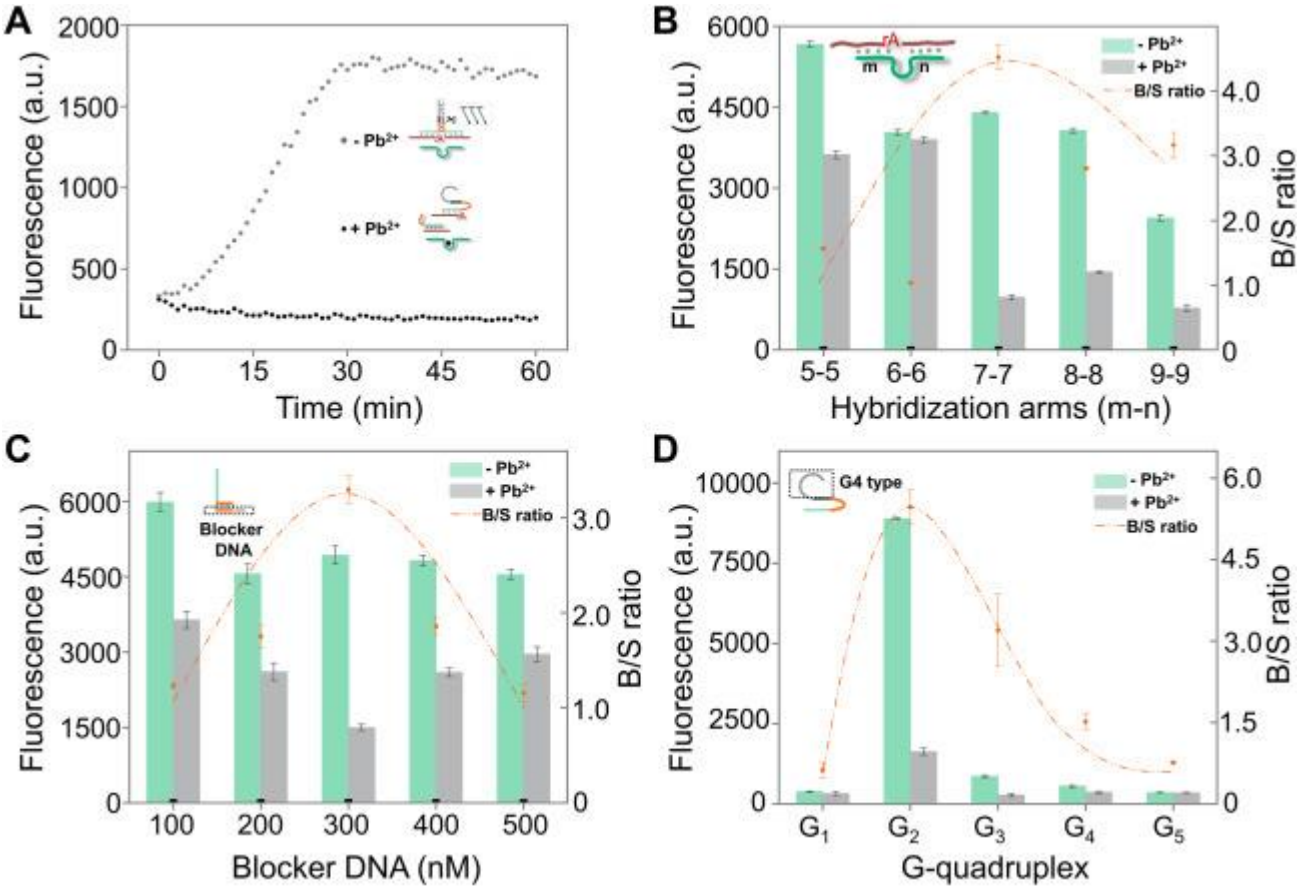

Fig. 4. Detection performance of the DNAzymee assay. (A) Fluorescent spectra in the presence of different concentrations of Pb^{2+} (0, 0.1, 0.2, 0.5, 3, 5, 10, 50, 100, 300, 500 nM). (B) The corresponding calibration curve of the fluorescence versus the concentration of Pb^{2+}. (C) The specificity of the DNAzymee assay for Pb^{2+} detection. The signal responded to various metal ions (Pb^{2+}, Cd^{2+}, Al^{3+}, Cu^{2+}, Mn^{2+}, Co^{2+}, and Ni^{2+}).

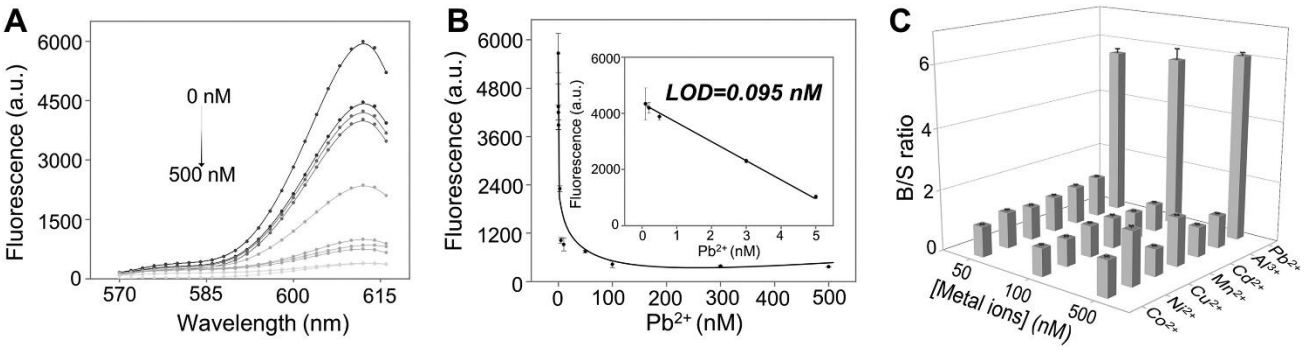

Fig. 5. Biosorbents screening and pH optimization using the DNAzymee assay. (A) Biosorption efficiency toward Pb2+ using ten bacteria at different pH conditions. Pb2+ concentration: 5 nM, biosorption time: 1 h, shaking condition: 150 r/min. FESEM images (magnification 100,000×, pH 7.0) of L. mesenteroides in the absence of Pb2+ (B) and presence of 50 μM (C), 100 μM (D), 200 μM (E) Pb2+. (F) Comparisons of FTIR spectra of L. mesenteroides in the absence of Pb2+ (I) and presence of 50 μM (II), 100 μM (III) and 200 μM Pb2+ (IV).

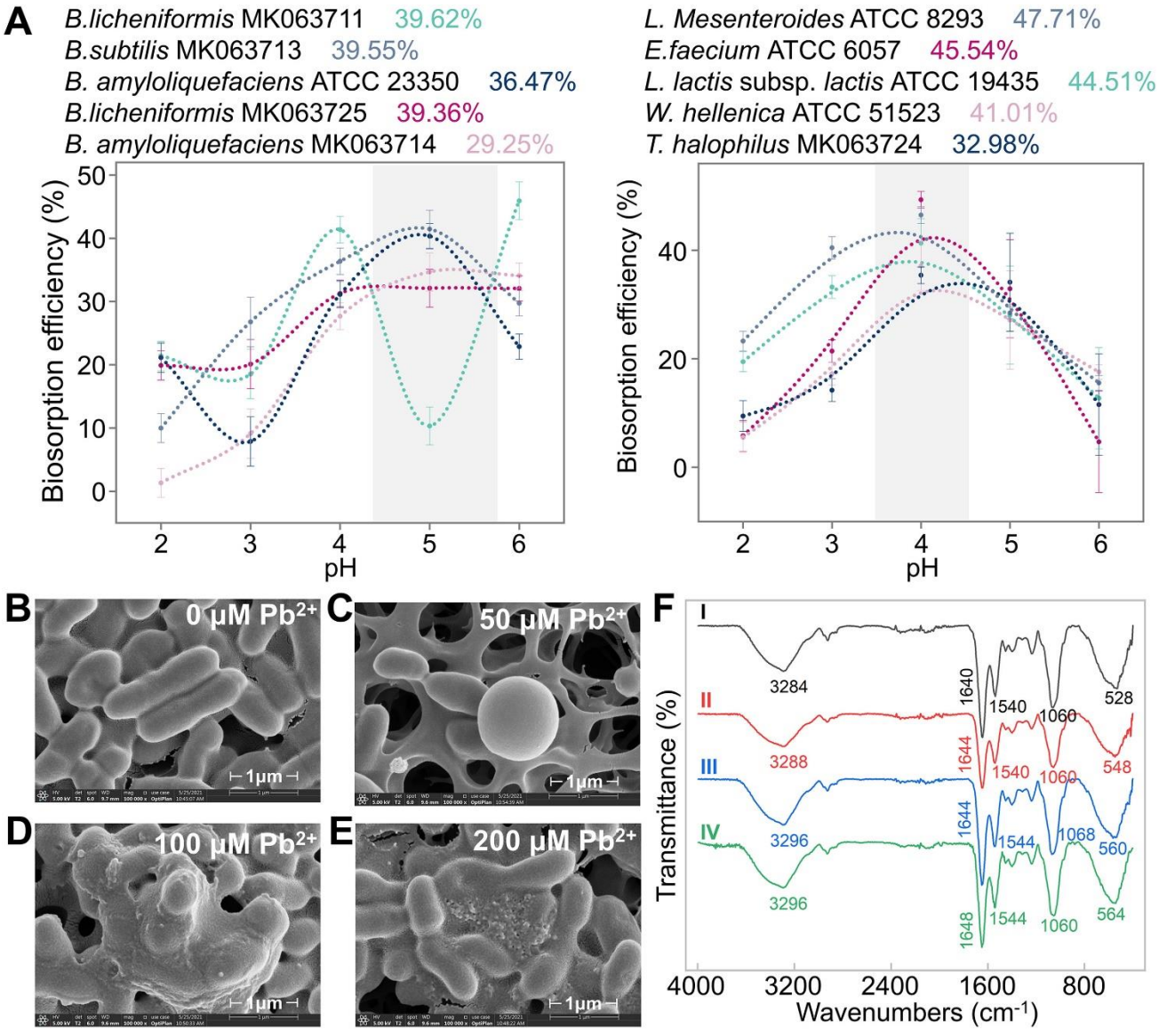

References

Ashraf, U., Mahmood, M.H.-u.-R., Hussain, S., Abbas, F., Anjum, S.A., Tang, X., 2020. Lead (Pb) distribution and accumulation in different plant parts and its associations with grain Pb contents in fragrant rice. Chemosphere 248, 126003. https://doi.org/10.1016/j.chemosphere.2020.126003.

Balasubramanian, B., Meyyazhagan, A., Chinnappan, A.J., Alagamuthu, K.K., Shanmugam, S.,Al-Dhabi, N.A., Mohammed Ghilan, A.K., Duraipandiyan, V., Valan, Arasu M., 2020. Occupational health hazards on workers exposure to lead (Pb): a genotoxicity analysis.J. Infect. Public Health 13 (4), 527–531. https://doi.org/10.1016/j.jiph.2019.10.005.

Breaker, R.R., Joyce, G.F., 1994. A DNA enzyme that cleaves RNA. Chem. Biol. 1 (4),223–229. https://doi.org/10.1016/1074-5521(94)90014-0.

Chen, X., Wang, X., Lu, Z., Luo, H., Dong, L., Ji, Z., Xu, F., Huo, D., Hou, C., 2020. Ultra-sensitive detection of Pb2+ based on DNAzymes coupling with multi-cycle strand dis-placement amplification (M-SDA) and nano-graphene oxide. Sensors Actuators B Chem.311, 127898. https://doi.org/10.1016/j.snb.2020.127898.

Concórdio-Reis, P., Reis, M.A.M., Freitas, F., 2020. Biosorption of heavy metals by the bacterialexopolysaccharide FucoPol. Appl. Sci. 10, 6708. https://doi.org/10.3390/app10196708.

Corroto, C., Iriel, A., Cirelli, A.F., Carrera, A.L.P., 2019. Constructed wetlands as an alternativefor arsenic removal from reverse osmosis effluent. Sci. Total Environ. 691, 1242–1250.https://doi.org/10.1016/j.scitotenv.2019.07.234.

Dai, Q.H., Bian, X.Y., Li, R., Jiang, C.B., Ge, J.M., Li, B.L., Ou, J., 2019. Biosorption of lead(II)from aqueous solution by lactic acid bacteria. Water Sci. Technol. 79 (4), 627–634.https://doi.org/10.2166/wst.2019.082.

Deng, R., Yang, H., Dong, Y., Zhao, Z., Xia, X., Li, Y., Li, J., 2018. Temperature-robustDNAzyme biosensors confirming ultralow background detection. ACS Sensors 3 (12),2660–2666. https://doi.org/10.1021/acssensors.8b01122.

Feng, Z., Zhang, W., Li, L., Tu, B., Ye, W., Tang, X., Wang, H., Xiao, X., Wu, T., 2021. A cost-effective detection of low-abundance mutation with DNA three-way junction structureand lambda exonuclease. Chin. Chem. Lett. 32 (2), 779–782. https://doi.org/10.1016/j.cclet.2020.06.009.

Halttunen, T., Salminen, S., Tahvonen, R., 2007. Rapid removal of lead and cadmium fromwater by specific lactic acid bacteria. Int. J. Food Microbiol. 114 (1), 30–35. https://doi.org/10.1016/j.ijfoodmicro.2006.10.040.

Inyang, M.I., Gao, B., Yao, Y., Xue, Y., Zimmerman, A., Mosa, A., Pullammanappallil, P., Ok,Y.S., Cao, X., 2016. A review of biochar as a low-cost adsorbent for aqueous heavymetal removal. Crit. Rev. Environ. Sci. Technol. 46 (4), 406–433. https://doi.org/10.1080/10643389.2015.1096880.

Kang, A., Mao, H., Li, B., Kou, C., Xu, X., Jahangiri, B., 2019. Investigation of selective filtration characteristics of filter media for pavement runoff treatment. J. Clean. Prod. 235,590–602. https://doi.org/10.1016/j.jclepro.2019.06.337.

Lan, T., Furuya, K., Lu, Y., 2010. A highly selective lead sensor based on a classic leadDNAzyme. Chem. Commun. 46 (22), 3896–3898. https://doi.org/10.1039/B926910J.

Li, X., Ming, Q., Cai, R., Yue, T., Yuan, Y., Gao, Z., Wang, Z., 2020. Biosorption of Cd2+ andPb2+ from apple juice by the magnetic nanoparticles functionalized lactic acid bacteriacells. Food Control 109, 106916. https://doi.org/10.1016/j.foodcont.2019.106916.

Liu, J., Hu, Q., Qi, L., Lin, J.-M., Yu, L., 2020. Liquid crystal-based sensing platform for detection of Pb2+ assisted by DNAzyme and rolling circle amplification. J. Hazard. Mater.400, 123218. https://doi.org/10.1016/j.jhazmat.2020.123218.

Lu, Y., Tan, X., Lv, Y., Yang, G., Chi, Y., He, Q., 2020. Physicochemical properties and microbial community dynamics during Chinese horse bean-chili-paste fermentation, revealedby culture-dependent and culture-independent approaches. Food Microbiol. 85,103309. https://doi.org/10.1016/j.fm.2019.103309.

Malavolti, M., Fairweather-Tait, S.J., Malagoli, C., Vescovi, L., Vinceti, M., Filippini, T., 2020.Lead exposure in an Italian population: food content, dietary intake and risk

assessment.Food Res. Int. 137, 109370. https://doi.org/10.1016/j.foodres.2020.109370.

Mohapatra, R.K., Parhi, P.K., Pandey, S., Bindhani, B.K., Thatoi, H., Panda, C.R., 2019. Activeand passive biosorption of Pb(II) using live and dead biomass of marine bacterium Bacillus xiamenensis PbRPSD202: kinetics and isotherm studies. J. Environ. Manag. 247,121–134. https://doi.org/10.1016/j.jenvman.2019.06.073.

Morillo Pérez, J.A., García-Ribera, R., Quesada, T., Aguilera, M., Ramos-Cormenzana, A.,Monteoliva-Sánchez, M., 2008. Biosorption of heavy metals by the exopolysaccharideproduced by Paenibacillus jamilae. World J. Microbiol. Biotechnol. 24 (11), 2699–2704. https://doi.org/10.1007/s11274-008-9800-9.

Pakdel, M., Soleimanian-Zad, S., Akbari-Alavijeh, S., 2019. Screening of lactic acid bacteria todetect potent biosorbents of lead and cadmium. Food Control 100, 144–150. https://doi.org/10.1016/j.foodcont.2018.12.044.

Pugazhendhi, A., Boovaragamoorthy, G.M., Ranganathan, K., Naushad, M., Kaliannan, T.,2018. New insight into effective biosorption of lead from aqueous solution usingRalstonia solanacearum: characterization and mechanism studies. J. Clean. Prod. 174,1234–1239. https://doi.org/10.1016/j.jclepro.2017.11.061.

Raevskii, O.A., Donskaya, Y.A., Antokhina, L.A., 1973. IR spectra and internal rotation relativeto the P-N bond of certain N-arylamidodichlorophosphates. Bull. Acad. Sci. USSR 22 (11),2438–2441. https://doi.org/10.1007/BF00926389.

Rao, H., Xue, X., Luo, M., Liu, H., Xue, Z., 2021. Recent advances in the development of colorimetric analysis and testing based on aggregation-induced nanozymes. Chin. Chem.Lett. 32 (1), 25–32. https://doi.org/10.1016/j.cclet.2020.09.017.

Rasmey, A.-H., Aboseidah, A.A., Youssef, A.K., 2018. Application of Langmuir and Freundlich isotherm models on biosorption of Pb2+ by freez-dried biomass of Pseudomonasaeruginosa. Egypt. J. Microbiol. 53 (1), 37–48. https://doi.org/10.21608/ejm.2018.2998.1050.

Roy Choudhury, P., Majumdar, S., Sahoo, G.C., Saha, S., Mondal, P., 2018. High pressure ultrafiltration CuO/hydroxyethyl cellulose composite ceramic membrane for separation ofCr (VI)

and Pb (II) from contaminated water. Chem. Eng. J. 336, 570–578. https://doi.org/10.1016/j.cej.2017.12.062.

Saran, R., Liu, J., 2016. A silver DNAzyme. Anal. Chem. 88 (7), 4014–4020. https://doi.org/10.1021/acs.analchem.6b00327.

Shan, Z., Lyu, M., Curry, D., Oakley, D., Oakes, K., Zhang, X., 2019. Cu-DNAzyme facilitateshighly sensitive immunoassay. Chin. Chem. Lett. 30 (9), 1652–1654. https://doi.org/10.1016/j.cclet.2019.05.037.

Yang, H., Li, F., Xue, T., Khan, M.R., Xia, X., Busquets, R., Gao, H., Dong, Y., Zhou, W., Deng,R., 2022. Csm6-DNAzyme tandem assay for one-pot and sensitive analysis of lead pollution and bioaccumulation in mice. Anal. Chem. 94 (48), 16953–16959. https://doi.org/10.1021/acs.analchem.2c04589.

Yang, Y., Yang, H., Wan, Y., Zhou, W., Deng, S., He, Y., He, G., Xie, X., Deng, R., 2021.Temperature-robust and ratiometric G-quadruplex proximate DNAzyme assay for robustly monitoring of uranium pollution and its microbial biosorbents screening.

J. Hazard. Mater. 413, 125383. https://doi.org/10.1016/j.jhazmat.2021.125383.Yi, Y.-J., Lim, J.-M., Gu, S., Lee, W.-K., Oh, E., Lee, S.-M., Oh, B.-T., 2017. Potential use of lac-tic acid bacteria Leuconostoc mesenteroides as a probiotic for the removal of Pb(II) tox-icity. J. Microbiol. 55 (4), 296–303. https://doi.org/10.1007/s12275-017-6642-x.

Zhang, Y., Wu, C., Liu, H., Khan, M.R., Zhao, Z., He, G., Luo, A., Zhang, J., Deng, R., He, Q.,2021. Label-free DNAzyme assays for dually amplified and one-pot detection of lead pollution. J. Hazard. Mater. 406, 124790. https://doi.org/10.1016/j.jhazmat.2020.124790.H. Yang et al. Science of the Total Environment 863 (2023) 1608997

Supporting Information

DNAzyme-templated exponential isothermal amplification for sensitive detection of lead pollution and high-throughput screening of microbial biosorbents

Hao Yang[a], Yumei Liu[a], Yi Wan[b], Yi Dong[a], Qiang He[a], Mohammad Rizwan Khan[c], Rosa Busquets[d], Guiping He[a], Jiaqi Zhang[a], Ruijie Deng[a], Zhifeng Zhao[a,*]

[a] College of Biomass Science and Engineering, Healthy Food Evaluation Research Center and Key Laboratory of Food Science and Technology of Ministry of Education of Sichuan Province, Sichuan University, Chengdu 610065, China

[b] Key Laboratory of Tropical Biological Resources of Ministry of Education, School of Life and Pharmaceutical Sciences, Marine College, State Key Laboratory of Marine Resource Utilization in South China Sea, Hainan University, Haikou 570228, China

[c] Department of Chemistry, College of Science, King Saud University, Riyadh, 11451, Saudi Arabia

[d] School of Life Sciences, Pharmacy and Chemistry, Kingston University, KT1 2EE Kingston Upon Thames, United Kingdom

* Corresponding authors:

e-mail: zhaozhifeng@scu.edu.cn

Table of Content

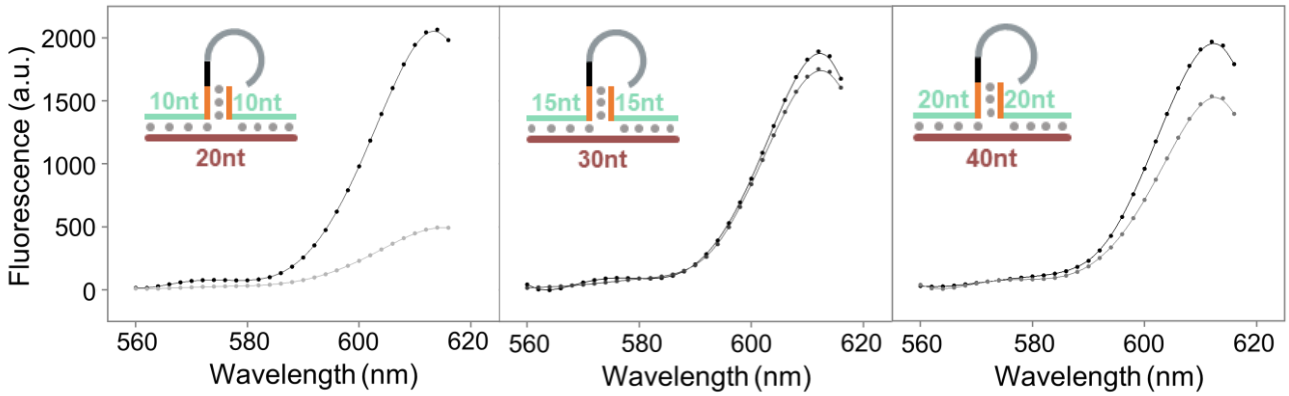

Fig. S1. Optimization of probes for EXPAR (P_1, P_2). The length of handle arms of P_1-P_2 were selected as 10-10 nt, 15-15 nt and 20-20 nt, respectively.

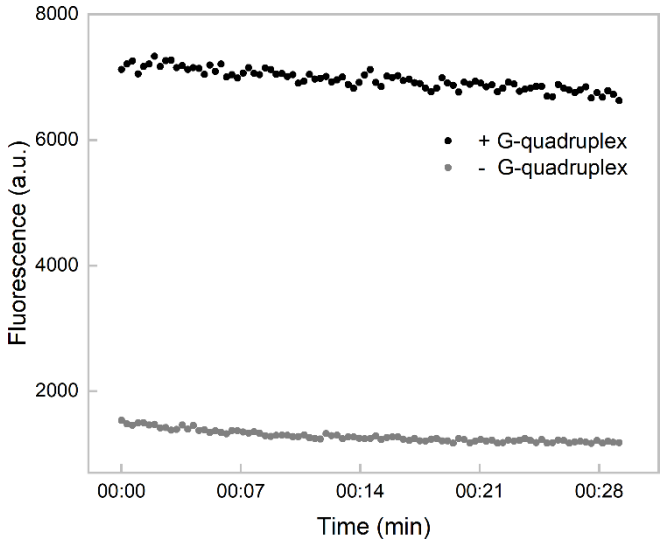

Fig. S2. Fluorescent dynamics in the presence and absence of G-quadruplex (G_2).

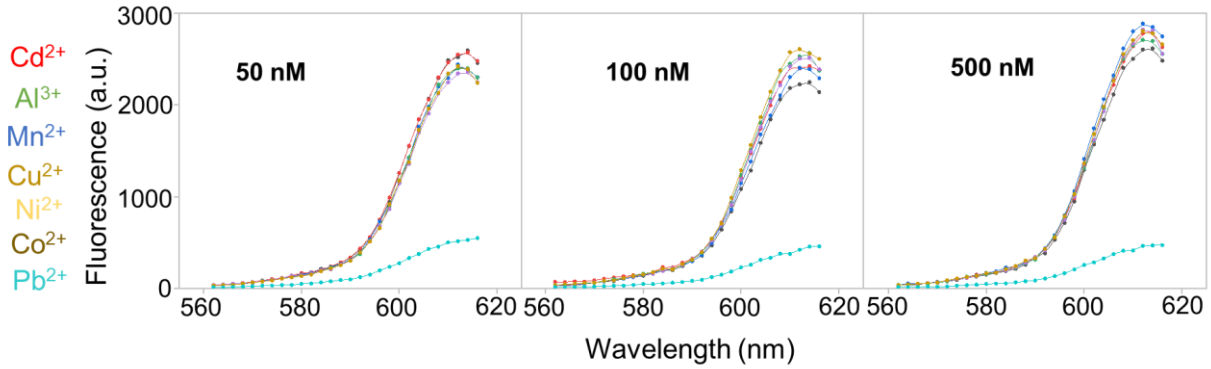

Fig. S3. Fluorescent analysis of the DNAzymee assay using different metal ions.

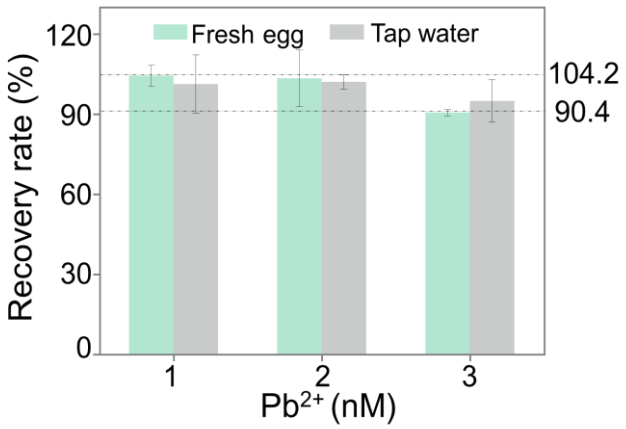

Fig. S4. Detection of Pb^{2+} in contaminant-spiked tap water and fresh egg samples. 1 nM, 2 nM, and 3 nM Pb^{2+} were added, respectively.

Table S1. Oligonucleotide sequences

Oligonucleotide	Sequences (5'-3')
Substrate strand	
Substrate	CTCACTATrAGGAAGAGATGATGTCTGT
Sub 1	GGAAGAGATGATGTCTGT
Sub 2	CTCACTATA
GR-5 DNAzyme strand	
5 nt – 5 nt	**TCTCT**GAAGTAGCGCCGCCG**TATAG**
6 nt – 6 nt	**ATCTCT**GAAGTAGCGCCGCCG**TATAGT**
7 nt – 7 nt	**CATCTCT**GAAGTAGCGCCGCCG**TATAGTG**
8 nt – 8 nt	**TCATCTCT**GAAGTAGCGCCGCCG**TATAGTGA**
9 nt – 9 nt	**ATCATCTCT**GAAGTAGCGCCGCCG**TATAGTGAG**
Probes for EXPAR	
P_1-10	*CATCTCTTCC*TTTCTACG
P_2-10	CCCACCCACCCACCCGCTGAGGCGTAGATT*TATAGTGAGA*
T10-10	TCTCACTATAGGAAGAGATG
P_1-15	*GACATCATCTCTTCC*TTTCTACG
P_2-15	CCCACCCACCCACCCGCTGAGGCGTAGATT*TATAGTGAGAAAAAA*
T15-15	TTTTTTCTCACTATAGGAAGAGATGATGTC
P_1-20	*AAACAGACATCATCTCTTCC*TTTCTACG
P_2-20	CCCACCCACCCACCCGCTGAGGCGTAGATT*TATAGTGAGAAAAAAAAAAA*
T20-20	TTTTTTTTTTTCTCACTATAGGAAGAGATGATGTCTGTTT
G-quadruplex probes	
G_1	AGGTTGGTGTGGTTGGA
G_2	GGGTGGGTGGGTGGG
G_3	GTGGGTAGGGCGGGTTGG
G_4	GGGTTTTGGGTTTTGGGTTTTGGG
G_5	GGGTTTTTTGGGTTTTTTGGGTTTTTTGGG
Blocker DNA	TTTTTTCGTAGA
Cleavage site	CCTCAGC

* The "rA" represents the adenosine ribonucleotide in the substrate. The bold parts are the hybridization arms of DNAzyme. The underlined italic parts are complementary parts between P_1, P_2 and the substrate.

Table S2. Bacterial strains used in this work

Strain name	Abbreviation	Accession number	Source
Bacillus subtilis	*B. subtilis*	MK063713 (NCBI)	Chinese Horse Bean-chili-paste
Bacillus licheniformis	*B. licheniformis*	MK063711 (NCBI)	Chinese Horse Bean-chili-paste
Bacillus licheniformis	*B. licheniformis*	MK063725 (NCBI)	Chinese Horse Bean-chili-paste
Bacillus amyloliquefaciens	*B. amyloliquefaciens*	MK063714 (NCBI)	Chinese Horse Bean-chili-paste
Bacillus amyloliquefaciens	*B. amyloliquefaciens*	ATCC 23350	Type strain
Lactococcus lactis subsp. *lactis*	*L. lactis* subsp. *lactis*	ATCC 19435	Type strain
Enterococcus faecium	*E. faecium*	ATCC 6057	Type strain
Leuconostoc mesenteroides	*L. mesenteroides*	ATCC 8293	Type strain
Weissella hellenica	*W. hellenica*	ATCC 51523	Type strain
Tetragenococcus halophiles	*T. halophiles*	MK063724 (NCBI)	Chinese Horse Bean-chili-paste

Table S3. Comparisons among different fluorescent biosensors for lead detection

Method	Recognition	Label-free	Linear range	LOD	Application	References
DNAzyme-templated EXPAR assay	**GR-5 DNAzyme**	**Yes**	**0.1-5 nM**	**0.095 nM**	**Screening of microbial biosorbents, tap water, egg, juice**	**This work**
Cas12-based DNAzyme	GR-5 DNAzyme	No	0.24-48 nM	0.48 nM	Water	*Anal. Chim. Acta,* 2022, 1192, 339356
Cas12a-G-quadruplex assay	G-quadruplex	No	0.1 nM-5 μM	2.6 nM	Tea beverage, milk	*Food Chem.*, 2022, 378, 131802
Cell free biosensor	Allosteric transcription factor	Yes	1-250 nM	0.1 nM	Water	*J. Hazard. Mater.*, 2022, 438, 129499
Nanoporous modified biosensor	G-quadruplex	Yes	50 nM-32 μM	12 nM	Sea water	*Sens. Actuators B Chem.*, 2020, 321, 128314
Ratiometric G-quadruplex assay	G-quadruplex	No	60-300 nM	28 nM	Fresh egg, tap water	*Biosensors*, 2021, 11, 274.
Sequential DNAzyme biosensor	GR-5 DNAzyme	No	0.1-10 nM	0.22 nM	Water, eggs	*ACS Sens.*, 2018, 3, 2660-2666
Tetrahedral DNA Nanostructure-based DNAzyme	GR-5 DNAzyme	No	0-500 nM	0.91 nM	Tobacco leaf extracts	*J. Clean. Prod.,* 2022, 362, 132544
Catalytic hairpin assembly-based DNAzyme	8-17 DNAzyme	No	0.5-1000 nM	0.5 nM	River water, grass carp	*Anal. Bioanal. Chem.*, 2022, 414, 6581

Table S4. Discrimination factor for different metal ions

Metal ions	50 nM	100 nM	500 nM
Mn^{2+}	11.70	4.55	4.86
Co^{2+}	54.78	8.32	8.21
Cu^{2+}	5.97	4.00	9.25
Cd^{2+}	3.39	8.23	293.52
Al^{3+}	18.35	9.37	6.00
Ni^{2+}	13.35	7.80	3.46

Table S5. Analysis of Pb^{2+} in water and fresh egg samples

Samples	Added (nM)	Found (nM)	Margin of error (nM)	Recovery (%)	RSD (%) n=3
Egg	1	1.04	0.07	104.24	3.91
	2	2.07	0.20	103.28	10.53
	3	2.71	0.02	90.40	1.14
Tap water	1	1.01	0.21	101.11	10.90
	2	2.04	0.05	101.95	2.67
	3	2.84	0.16	94.82	7.94

Table S6. Determination of the average amount of Pb^{2+} biosorption per bacterial cell

Bacteria species	Average amount of Pb^{2+} biosorption per bacterial cell (fM / cell)
T. halophilus (MK063724)	1.69 ± 0.067
L. lactis subsp. lactis (ATCC 19435)	2.23 ± 0.076
W. hellenica (ATCC 51523)	2.05 ± 0.022
L. mesenteroides (ATCC 8293)	2.43 ± 0.046
E. Faecium (ATCC 6057)	1.82 ± 0.034
B. licheniformis (MK063711)	1.98 ± 0.029
B. licheniformis (MK063725)	1.46 ± 0.089
B. amyloliquefaciens (ATCC 23350)	1.98 ± 0.067
B. amyloliquefaciens (MK063714)	1.35 ± 0.098
B. subtilis (MK063713)	1.49 ± 0.020

Table S7. Comparisons of efficiency of Pb^{2+} biosorption with different biosorbents

Species	Optimal pH	Biomass concentration (g/L)	biosorption time (h)	Removal efficiency (%)	Type of sample	References
L. mesenteroides	**4.0**	**1**	**1**	**48**	**Pear juice**	**This work**
Chaetoceros sp.	6.0	1.5	3	60	Spiked water	*J. Community Health Res.*, 2015, 4(2), 114
Bacillus xiamenensis	6.0	1	24	90	Water	*J. Environ. Manage.*, 2019, 247, 121
Cyanothece sp.	5.0-6.0	1	1	62	Spiked water	*J. of Env. Chem. Eng.*, 2016, 4(2), 2529
Lactobacillus brevis	6.0	1	10	47	Spiked water	*J. Water Sci. and Technol.*, 2019, 79(4), 627
Neochloris minuta	5.0	1	1	67	Spiked water	*Appl. Water Sci.*, 2021, 11(2), 39